Table 4.2.1.7. *Intensity gain with storage rings over conventional sources; from Farge & Duke (1979), courtesy of ESF*

	GX6 rotating-anode tube 2.4 kW (Cu $K\alpha$ emission)	DCI 1.72 GeV and 240 mA	ESRF 5 GeV and 565 mA
Brightness impact ▲	Small-angle scattering with a double monochromator	×500 to 1000	×15000 to 3000
	Protein crystallography with a single-focus monochromator 1 mm^3 samples Small samples	 ×50 to 160 ×30 to 60	 ×900 to 1800 ×650 to 1300
	Diffuse scattering (wide angles, low resolution and large samples) with a curved graphite monochromator	×20 to 40	×160 to 320
Non characteristic wavelength (continuous background) EXAFS experimental set-up with a 100 kW rotating anode		×10^4	×10^5

Channelling radiation, resulting from the incidence of electrons with an energy of only about 5 MeV on appropriately aligned diamond or silicon crystals hold out the hope of producing a bright tunable X-ray source.

One or more of these methods may, in the future, be developed as X-ray sources that can compete with synchrotron-radiation sources.

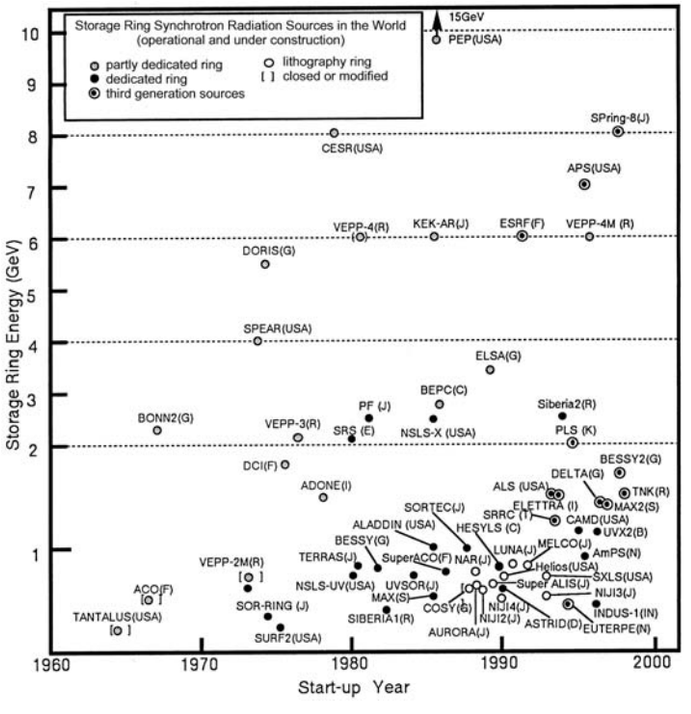

Fig. 4.2.1.11. The evolution of storage-ring synchrotron-radiation sources over the decades, as illustrated by their increasing number and range of machine energies (based on Suller, 1992).

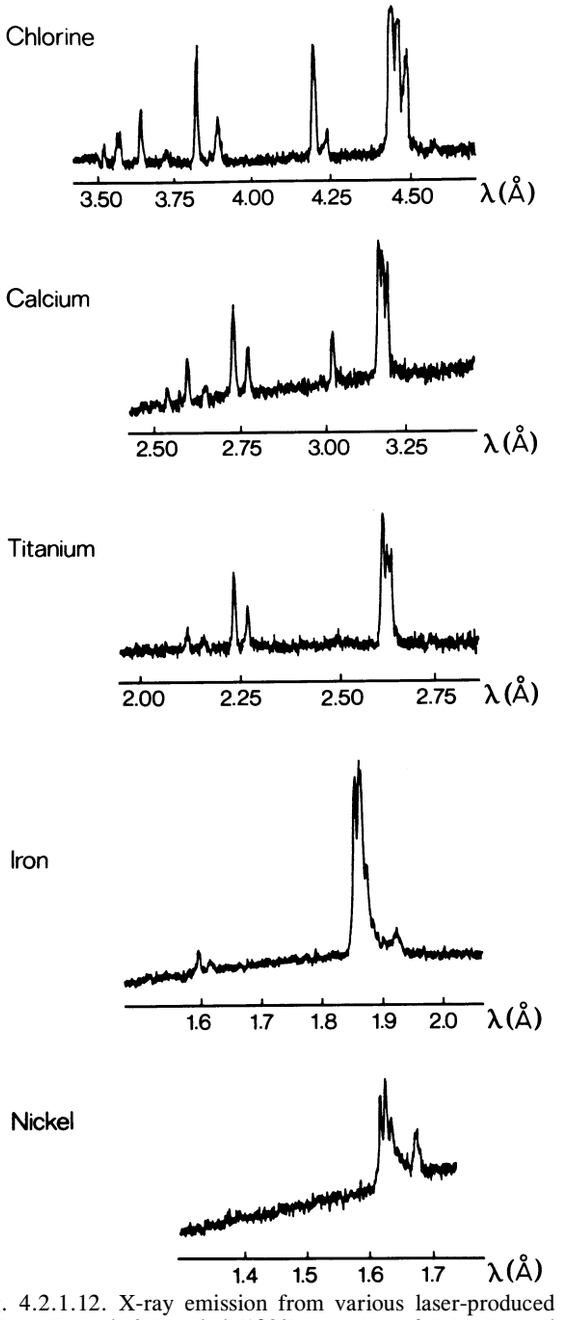

Fig. 4.2.1.12. X-ray emission from various laser-produced plasmas. From Forsyth & Frankel (1980); courtesy of J. M. Forsyth.

4.2.2. X-ray wavelengths (By R. D. Deslattes, E. G. Kessler Jr, P. Indelicato, and E. Lindroth)

4.2.2.1. *Historical introduction*

Wavelength tables in previous editions of this volume (Rieck, 1962; Arndt, 1992) were mainly obtained from the compilations prepared in Paris under the general direction of Professor Y. Cauchois (Cauchois & Hulubei, 1947; Cauchois & Senemaud, 1978). A separate effort by the late Professor J. A. Bearden and his collaborators (Bearden, 1967) has been widely used in other aggregations of tabular data and was made available for some time through the Standard Reference Data Program at the National Institute of Standards and Technology (NIST). For simplicity in the following discussion, we use the Bearden database as a frame of reference with respect to which our

current, and rather different, approach can be compared. Although a detailed comparison of the historical databases may be of some interest, the result would have only very small influence on the outcome presented here. To specify this framework, we begin with a brief description of the procedures used in establishing this reference database.

Bearden and his collaborators remeasured a group of five X-ray lines (Bearden, Henins, Marzolf, Sauder & Thomsen, 1964), with the remaining entries in the wavelength table coming from a critically reviewed, and re-scaled, subset of earlier measurements (Bearden, 1967). Line locations were given in Å* units, a scale defined by setting the wavelength of W $K\alpha_1 = 0.2090100$Å*. It was Bearden's intention that, for all but the most demanding applications, one could simply assign Å*/Å $= 1$, with an uncertainty arising from the fundamental physical constants, particularly N_A and hc/e, combined with uncertainties arising from the measurement technology (Bearden, 1965). Not long after the publication of the final compilation (Bearden, 1967), it became clear that the fundamental constants used in defining Å* needed significant revision (Cohen & Taylor, 1973), and that there were some inconsistencies in the metrology (Kessler, Deslattes & Henins, 1979).

4.2.2.2. *Known problems*

Aside from the particular issues noted above, all previous wavelength tables had certain limitations arising from the procedures used in their generation. In particular, except for a small group of five $K\alpha$ spectra (Bearden, Thomsen *et al.*, 1964), the Bearden tables relied entirely on data previously reported in the literature. Both of the other tabulations also proceeded using only reported experimental values (Cauchois & Hulubei, 1947; Cauchois & Senemaud, 1978). In the Bearden compilation process, available data for each emission line were weighted according to claimed uncertainties, modified in certain cases by Bearden's detailed knowledge of the measurement practices of the major sources of experimental wavelength values. The complete documentation of this remarkable undertaking is, unfortunately, not widely accessible. Our evident need to understand the origin of the 'recommended' values has been greatly aided by the availability of a copy of the full documentation (Bearden, Thomsen *et al.*, 1964).

The actual experimental data array from which the previous tables emerged is not complete, even for the prominent ('diagram') lines. In the cases where experimental data were not available [as can be seen only in the source documentation (Bearden, Thomsen *et al.*, 1964)], the gaps were filled by interpolated values based on measurements available from nearby elements, plotted on a modified Moseley diagram in which the Z^2 term dependence is taken into account (Burr, 1996). In the end, such a smooth scaling with respect to nuclear charge suppresses the effects of the atomic shell structure, a practice that must be avoided in order to obtain the significant improvement in the database that we hope to provide. Also obscured in smooth Z scaling are detectable contributions arising from the fact that nuclear sizes do not change smoothly as a function of the nuclear charge, Z.

4.2.2.3. *Alternative strategies*

There are several possible approaches to generating an improved, 'all-Z' table of X-ray wavelengths. These range from the option of conducting a massive measurement campaign to populate more fully the currently available tabular array to a large computational endeavor that might purport to carry out multiconfiguration, relativistic wavefunction calculations for the entire Periodic Table. It seems evident to us that there is little interest in, and even less support for, mounting the large effort needed to realize an improved tabulation of X-ray wavelengths by purely experimental means, while the possibility of proceeding in an entirely theoretical mode is not consistent with the evident need that at least some wavelengths be reported with uncertainties that approach the limit of what can be obtained from the naturally occurring X-ray lines. The actual location of any useful feature of a line is influenced not only by the physical and chemical environment of the emitting atom but also by inevitable multi-electron excitation processes that perturb the entire spectral profile. Calculation of such complexities currently lies beyond the limits of practicality, eliminating the option of proceeding without strong coupling to experimental profile locations, at least for crystallographically important X-ray lines. Similar considerations apply *a fortiori* to those lines needed as reference wavelengths for exotic atom measurements, such as those leading to masses of elementary particles and tests of basic theory [see *e.g.* Beyer, Indelicato, Finlayson, Liesen & Deslattes (1991)].

In constructing the accompanying tables, we have chosen a new procedure that differs from those described above, and accordingly requires some detailed commentary. We begin with the presently available network of well documented experimental measurements, originally established to provide a test bed for the theoretical methods developing at that time (Deslattes & Kessler, 1985). This modest network was the first compilation to make use of the, then newly available, connection between the X-ray region and the base unit of the International System of measurement (the SI) based on optical interferometric measurement of a lattice period as revealed by X-ray interferometry. Details of the generation of this network and its subsequent expansion will be given below. Using this network as a test set gave clearer suggestions as to specific limitations of the theoretical modelling than had been evident from using other, less selective, experimental reference compilations available at that time. Extensive theoretical developments before and, especially, after the appearance of this new experimental reference set have shown a steady convergence toward these critically evaluated data. Following this evolution further, our long-term plan is to use these new theoretical calculations to provide a more structured and accurate interpolation procedure for estimating the spectra of elements lying between those for which we have accurate measurements, or spectra well connected to a directly established reference wavelength. The present table provides experimental and theoretical values for some of the more prominent K and L series lines and is a subset of a larger effort for all K and L series lines connecting the $n = 1$ to $n = 4$ shells. The more complete table will be published elsewhere and be made available on the the NIST Physical Reference Data web site. In addition, experimental values for the K and L edges are provided. Although the reference data are inadequate in both low and high ranges of Z, the general consistency of theory and experiment through the region $20 < Z < 90$ for the strong K-series and L-series lines suggests that, in the absence of good reference measurements, the uncorrected theoretical values should be considered for applications not requiring the highest accuracy.

4.2.2.4. *The X-ray wavelength scales, old and new*

Historically, from the first realizations of refined spectroscopy in the X-ray region (*ca* 1915–1925) up to the period 1975–1985, the best measured X-ray wavelengths had to be expressed in some local unit, most often designated as the xu (x unit) or kxu

(kilo x unit). Uncertainty in the conversion factor between the X-ray and optical scales was the dominant contributor to the total uncertainties in the wavelength values of the sharper X-ray emission lines, such as those most frequently used in crystallography. (For a discussion of the present values in relation to previously assigned numerical values on the various scales, see Subsection 4.2.2.14.) This local unit was, for most of the time, 'officially' defined by assigning a specific numerical value to the lattice period of a particular reflection from 'the purest instance' of a particular crystal. Originally this was rocksalt; later it was calcite. In practice, most work used as *de facto* standards certain values for Cu $K\alpha_1$ and Mo $K\alpha_1$ whose inconsistency, though noted by some crystallographers earlier, was seriously addressed by Bearden and co-workers only in the 1960's (Bearden, Henins *et al.*, 1964). This early history was summarized in 1968 (Thomsen & Burr, 1968). Connection of the X-ray wavelength scale to the primary realizations of the length (wavelength) unit in the 'metric system' was primarily (at least after about 1930) through ruled grating measurements of longer-wavelength X-ray lines such as Al $K\alpha_{1,2}$.

The remainder of the X-ray wavelength database was derived from relative measurements using crystal diffraction spectroscopy. Unfortunately, even the most refined among the ruled grating measurements did not give accuracies comparable to the precision accessible by relative wavelength measurements (Henins, 1971). As noted above, in connection with establishing the previous wavelength table, Bearden introduced a new local unit, the Å*, based on an explicit value for the wavelength of W $K\alpha_1$, chosen to give a conversion factor near unity. This transitional period will not be treated further in the present documentation since, to a substantial extent, developments described in the following paragraphs have effectively eliminated the need for a local scale for X-ray wavelength metrology.

Following the demonstration of crystal lattice interferometry in the X-ray region (Bonse & Hart, 1965), efforts to combine such an X-ray interferometer with various optical interferometers were undertaken in several (mostly national standards) laboratories. Although the earliest of these, carried out at the National Bureau of Standards (NBS) (now the National Institute of Standards and Technology, NIST) (Deslattes & Henins, 1973) was, in the end, found to be burdened by a serious systematic error (1.8×10^{-6}) in later work at the Physikalisch Technishe Bundesanstalt (PTB) (Becker *et al.*, 1981; Becker, Seyfried & Siegert, 1982), it was clear that accuracy limitations associated with ruled grating measurements no longer dominated the metrology of X-ray wavelengths. The origin of the systematic error in the early NBS measurement was subsequently understood (Deslattes, Tanaka, Greene, Henins & Kessler, 1987), and, more recently, excellent results were obtained in Italy (Basile, Bergamin, Cavagnero, Mana, Vittone & Zosi, 1994, 1995) and Japan (Fujimoto, Fujii, Tanaka & Nakayama, 1997). In all cases, the goal was to obtain an optical measurement of a crystal lattice period (thus far, only Si 220) and to use the calibrated crystals in diffraction spectrometry to establish optically based X-ray wavelengths. Such exercises have been undertaken for several X-ray lines, but the most detailed and well documented results to date were obtained in Jena (Härtwig, Hölzer, Wolf & Förster, 1993; Hölzer, Fritsch, Deutsch, Härtwig & Förster, 1997), where the $K\alpha$ and $K\beta$ spectra of the elements Cr to Cu were evaluated using silicon crystals well connected with the crystal spacings measured at the PTB.

4.2.2.5. *K-series reference wavelengths*

In addition to the Jena measurements noted above, a number of characteristic X-ray lines were measured on the optically based scale at NBS/NIST. The set of directly measured reference wavelengths is given in Table 4.2.2.1 in bold type. Most of the originally published (NBS/NIST) values were burdened by the 1.8×10^{-6} error in the silicon lattice period, as noted above. These have been corrected in the numerical results summarized in the table. The directly measured elements and lines appearing in this table were often chosen to meet the need for specific reference values in locations near those of certain optical transitions in highly charged ion spectra or spectra from pionic atoms. In addition, early NBS measurements specifically addressed the lines most often used in crystallography and the W $K\alpha$ transition. In response to the needs of electron spectroscopy, Al and Mg K spectra were also determined (Schweppe, Deslattes, Mooney & Powell, 1994). In this case, the original lattice error had been previously recognized, so that no rescaling was required. The remaining directly measured entries were obtained as opportunities to do so emerged.

The optically based data set was expanded by noting that several groups of accurate (relative) measurements in the literature either contained one of the directly measured lines (bold type) in Table 4.2.2.1 or were explicitly connected to one of them. Most often this situation was realized in reports that indicated a specific reference value, *i.e.* where it was stated numerical values are based on a scale where, for example, the wavelength of Mo $K\alpha_1$ was taken as 707.831 xu. In such cases, and where other indicators of good measurement quality are presented, it is easy to re-scale the data reported so that it is consistent with the optically based data. This procedure was followed for important groups of measurements from earlier work by Bearden and co-workers, and from the X-ray laboratory at Uppsala. The rescaled numerical results are included in Table 4.2.2.1 in normal type along with the specific literature citations. The indicated uncertainties are standard uncertainties as defined by ISO (Taylor & Kuyatt, 1994; Schwarzenbach, Abrahams, Flack, Prince & Wilson, 1995).

4.2.2.6. *L-series reference wavelengths*

To date, only a very limited number of L-series emission lines have been directly measured on an optically based scale. Wavelengths for directly measured L-series lines are reported in Table 4.2.2.2 along with the literature citations. In the future, we hope to expand this limited data set by including other lines and elements that are well connected to these reference lines in the literature.

4.2.2.7. *Absorption-edge locations*

Only a small number of absorption-edge locations have been directly measured to high accuracy using the currently acceptable protocols. Some of the available data were obtained in order to provide wavelength determinations for spectra from highly charged and/or exotic atoms (Bearden, 1960; Lum *et al.*, 1981). This small group was, however, significantly expanded very recently by an important set of new measurements, extending to $Z = 51$, that are well coupled to the optical wavelength scale (Kraft, Stümpel, Becker & Kuetgens, 1996) The resulting experimental database is summarized in Table 4.2.2.3. The effort that would be needed to expand the experimental database in a systematic way is quite large. Thus, we make use of a procedure, not previously used for this purpose, that combines available electron binding energy data with emission-line locations from our expanded reference set of emission-line data and emission lines that have been rescaled to be consistent with the optically based scale. At the same time, calculation of the location of absorption thresholds within the

Table 4.2.2.1. *K-series reference wavelengths in Å; bold numbers indicate a directly measured line*

Numbers in parentheses are standard uncertainties in the least-significant figures.

Z	Symbol	A	$K\alpha_2$	$K\alpha_1$	$K\beta_3$	$K\beta_1$	References
12	Mg		**9.89153 (10)**	**9.889554 (88)**			(*a*)
13	Al		**8.341831 (58)**	**8.339514 (58)**			(*a*)
14	Si		**7.12801 (14)**	**7.125588 (78)**			(*b*)
16	S		**5.374960 (89)**	**5.372200 (78)**			(*b*)
17	Cl		**4.730693 (71)**	**4.727818 (71)**			(*b*)
18	Ar		**4.194939 (23)**	**4.191938 (23)**			(*c*)
19	K		**3.7443932 (68)**	**3.7412838 (56)**			(*d*)
24	Cr		**2.2936510 (30)**	**2.2897260 (30)**	**2.0848810 (40)**	**2.0848810 (40)**	(*e*)
25	Mn		**2.1058220 (30)**	**2.1018540 (30)**	**1.9102160 (40)**	**1.9102160 (40)**	(*e*)
26	Fe		**1.9399730 (30)**	**1.9360410 (30)**	**1.7566040 (40)**	**1.7566040 (40)**	(*e*)
27	Co		**1.7928350 (10)**	**1.7889960 (10)**	**1.6208260 (30)**	**1.6208260 (30)**	(*e*)
28	Ni		**1.6617560 (10)**	**1.6579300 (10)**	**1.5001520 (30)**	**1.5001520 (30)**	(*e*)
29	Cu		**1.54442740 (50)**	**1.54059290 (50)**	**1.3922340 (60)**	**1.3922340 (60)**	(*e*)
31	Ga		**1.3440260 (40)**	**1.3401270 (96)**	1.208390 (75)	1.207930 (34)	(*b*),(*f*)
33	As		**1.108830 (31)**	**1.104780 (12)**	0.992689 (79)	0.992189 (53)	(*b*),(*f*)
34	Se		1.043836 (30)	**1.039756 (30)**	0.933284 (74)	0.932804 (30)	(*b*),(*f*)
36	Kr		**0.9843590 (44)**	**0.9802670 (40)**	**0.8790110 (70)**	**0.8785220 (50)**	(*b*)
40	Zr		**0.7901790 (25)**	**0.7859579 (27)**	**0.7023554 (30)**	**0.7018008 (30)**	(*b*)
42	Mo		0.713607 (12)	**0.70931715 (41)**	0.632887 (13)	0.632303 (13)	(*d*),(*f*)
44	Ru		0.6474205 (61)	0.6430994 (61)	0.5730816 (42)	0.5724966 (42)	(*d*),(*f*)
45	Rh		0.6176458 (61)	0.6132937 (61)	0.5462139 (42)	0.5456189 (42)	(*d*),(*f*)
46	Pd		0.5898351 (60)	0.5854639 (46)	0.5211363 (41)	0.5205333 (41)	(*d*),(*f*)
47	Ag		**0.5638131 (26)**	**0.55942178 (76)**	0.4976977 (60)	0.4970817 (60)	(*d*),(*f*)
48	Cd		0.5394358 (46)	0.5350147 (46)	0.4757401 (71)	0.4751181 (71)	(*d*),(*f*)
49	In		0.5165572 (60)	0.5121251 (46)	0.4551966 (41)	0.4545616 (41)	(*d*),(*f*)
50	Sn		0.4950646 (46)	0.4906115 (46)	0.4358821 (51)	0.4352421 (51)	(*d*),(*f*)
51	Sb		0.4748391 (45)	0.4703700 (45)	0.4177477 (41)	0.4170966 (31)	(*d*),(*f*)
54	Xe		**0.42088103 (71)**	**0.4163508 (14)**	**0.3694051 (13)**	**0.3687346 (13)**	(*d*)
56	Ba		**0.38968378 (74)**	**0.38512464 (84)**	**0.3415228 (11)**	**0.34082708 (75)**	(*d*)
60	Nd		**0.3248079 (59)**	**0.3201648 (59)**	0.283634 (59)	0.282904 (44)	(*d*),(*f*)
62	Sm		**0.31369830 (79)**	**0.30904506 (46)**	0.273764 (30)	0.273014 (30)	(*d*),(*f*)
67	Ho		0.26549088 (84)	0.2607608 (42)	0.230834 (30)	0.230124 (30)	(*f*),(*g*)
68	Er		**0.2571133 (11)**	**0.25237359 (62)**	**0.2234766 (14)**	**0.22269866 (72)**	(*d*)
69	Tm		0.24910095 (61)	0.24434486 (44)	0.216366 (30)	0.21559182 (57)	(*f*),(*h*)
74	W		0.21383304 (50)	**0.20901314 (18)**	0.18518317 (70)	0.1843768 (30)	(*d*),(*f*)
79	Au		**0.18507664 (61)**	**0.18019780 (47)**	**0.1598249 (13)**	**0.15899527 (77)**	(*d*)
82	Pb		**0.17029527 (56)**	**0.16537816 (38)**	**0.1468129 (10)**	**0.14596836 (58)**	(*d*)
83	Bi		0.1657183 (20)	0.1607903 (46)	0.142780 (11)	0.1419492 (54)	(*f*),(*g*)
90	Th	230	**0.13782600 (31)**	**0.13282021 (36)**	**0.11828686 (78)**	**0.11740759 (59)**	(*d*)
91	Pa	231	0.1343516 (29)	0.1293302 (27)	0.1152427 (21)	0.1143583 (21)	(*i*)
92	U	238	**0.13099111 (78)**	**0.12595977 (36)**	**0.11228858 (66)**	**0.11140132 (65)**	(*d*)
93	Np	237	0.1277287 (39)	0.1226882 (36)	0.1094230 (39)	0.1085265 (28)	(*i*)
94	Pu	239	0.1245782 (15)	0.11952120 (69)			(*h*)
94	Pu	244	0.1245705 (25)	0.1195140 (23)	0.1066611 (18)	0.1057595 (18)	(*i*)
95	Am	243	0.1215158 (24)	0.1164463 (33)	0.1039794 (17)	0.1030803 (17)	(*i*)
96	Cm	248	0.1185427 (23)	0.1134635 (21)	0.1013753 (17)	0.1004708 (16)	(*i*)
97	Bk	249	0.1156630 (54)	0.1105745 (49)	0.0988598 (55)	0.0979514 (54)	(*i*)
98	Cf	250	0.1128799 (82)	0.1077793 (75)			(*i*)

References: (*a*) Schweppe *et al.* (1994); (*b*) Mooney (1996); (*c*) Schweppe (1995); (*d*) Deslattes & Kessler (1985); (*e*) Hölzer *et al.* (1997); (*f*) Bearden (1967); (*g*) Borchert, Hansen, Jonson, Ravn & Desclaux (1980); (*h*) Borchert (1976); (*i*) Barreau, Börner, Egidy & Hoff (1982).

theoretical framework (see below) has been undertaken and will be made available in the longer publication and on the web site.

The feature of absorption spectra customarily designated as 'the absorption edge' has been variously associated with: the first inflection point of the absorption spectrum; the energy needed to produce a single inner vacancy with the photo-electron 'at rest at infinity'; or the energy needed to remove an electron from an inner shell and place it in the lowest unoccupied energy level. A general discussion of this question has been given by Parratt (1959). If we choose the second alternative, then it is easy to see that, with some care for symmetry restrictions, one can estimate the absorption-edge energy by combining the binding energy for any accessible outer shell with the energy of an emission line for which the transition terminus lies in the same outer shell. Of course, this procedure does not focus on the details of absorption thresholds, the locations of which are important for a number of structural applications. On the other hand, our choice gives greater regularity with respect to nuclear charge and facilitates use of electron binding energies, since they are referenced to the Fermi energy or the vacuum.

Electron binding energies have been tabulated for the principal electron shells of all the elements considered in the present table (Fuggle, Burr, Watson, Fabian & Lang, 1974; Cardona & Ley, 1978; Nyholm, Berndtsson & Mårtensson,

Table 4.2.2.2. *Directly measured L-series reference wavelengths in Å*

Numbers in parentheses are standard uncertainties in the least-significant figures.

Z	Symbol	$L\alpha_2$	$L\alpha_1$	$L\beta_1$	References
36	Kr	7.82032(13)	7.82032(13)	7.574441(98)	(*a*)
40	Zr	6.07710(48)	6.070250(79)	5.836214(76)	(*a*)
54	Xe	3.025940(22)	3.016582(15)	2.806553(19)	(*b*)
60	Nd	2.38079(52)	2.370526(16)	2.167008(19)	(*a*)
62	Sm	2.210430(24)	2.199873(13)	1.998432(30)	(*a*)
67	Ho	1.856472(15)	1.845092(17)	1.647484(32)	(*a*)
68	Er	1.795701(45)	1.784481(20)	1.587466(86)	(*a*)
69	Tm	1.738003(19)	1.7267720(70)	1.5302410(70)	(*a*)

References: (*a*) Mooney (1996); (*b*) Mooney *et al.* (1992).

1980; Nyholm & Mårtensson, 1980; Lebugle, Axelsson, Nyholm & Mårtensson, 1981; Powell, 1995). The number of values available offers the possibility of consistency checking, since the K and L shells are connected by emission lines to several final hole states, each of which has (possibly) been evaluated by photoelectron spectroscopy. For each of the elements for which well qualified reference spectra are available, we evaluated edge location estimates using several alternative transition cycles and used the distribution of results to provide a measure of the uncertainty. Comparison of edge estimates obtained by this procedure with experimental data provides a quantitative test of the utility of the chosen approach to edge location estimation. In Table 4.2.2.3, the numerical results in the column labelled 'Emission + binding energies' were obtained by combining emission energies and electron binding energies using all possible redundancies. The estimated uncertainties indicated were obtained from the distribution of the redundant routes. As can be seen, the results are in general agreement with the available directly measured values. Accordingly, we have used this protocol to obtain the edge locations listed in the summary tables below.

4.2.2.8. *Outline of the theoretical procedures*

Only recently has it become possible to understand the relativistic many-body problem in atoms with sufficient detail to permit meaningful calculation of transition energies between hole states (Indelicato & Lindroth, 1992; Mooney, Lindroth, Indelicato, Kessler & Deslattes, 1992; Lindroth & Indelicato, 1993, 1994; Indelicato & Lindroth, 1996). To deal with those hole states for atomic numbers ranging from 10 to 100, one needs to consider five kinds of contributions, all of which must be calculated in a relativistic framework, and the relative influence of which can change strongly as a function of the atomic number:

(i) nuclear size;

(ii) relativistic effects (corrections to Coulomb energy, magnetic and retardation energy);

(iii) Coulomb and Breit correlation;

(iv) radiative (QED) corrections (one- and two-electron Lamb shift *etc.*);

(v) Auger shift.

Such an undertaking, although much more advanced than any other done in the past, still suffers from severe limitations that need to be understood fully to make the best use of the table. The main limitation is probably that most lines are emitted by atoms in an elemental solid or a compound, while the calculation at present deals only with atoms isolated in vacuum. (A purely experimental database would have a similar limitation.) The second limitation is that it is not possible at present to include the coupling between the hole and open outer shells. Coupling between a $j = \frac{1}{2}$, $j = \frac{3}{2}$ or $j = \frac{5}{2}$ hole and an external $3d$ or $4f$ shell can generate hundreds of levels, with splitting that can reach an eV. One then should calculate all radiative and Auger transition probabilities between hundreds of initial and final states. (The Auger final state would have one extra vacancy, leading eventually to thousands of final states.) Such an approach would give not only the mean line energy but also its shape and would thus be very desirable, but is impossible to do with present day theoretical tools and computers. We have thus limited ourselves to an approach in which one computes the weighted average energy for each hole state, and ignores possible distortion of the line profile due to the coupling between inner vacancies and outer shells.

Since we want to have good predictions for both light and heavy atoms, we have to include relativity non-perturbatively. To get a result approaching 1×10^{-6} for uranium $K\alpha$ by applying perturbation theory to the Schrödinger equation, for example, one would need to go to order 22 in powers of $Z\alpha = v/c$. The natural framework in this case is thus to do a calculation exact to all orders in $Z\alpha$ by using the Dirac equation. We thus have used many-body methods, based on the Dirac equation, in which the main contributions to the transition energy are evaluated using the Dirac–Fock method. We use the Breit operator for the electron–electron interaction, to include magnetic (spin–spin, spin–other orbit and orbit–orbit interactions in the lower orders in $Z\alpha$ and $(v/c)^2$ retardation effects. Higher-order retardation effects are also included.

Table 4.2.2.3. *Directly measured and emission + binding energies (see text) K-absorption edges in Å*

Numbers in parentheses are standard uncertainties in the least significant figures.

Z	Symbol	Directly measured	Emission + binding energies	References
23	V	2.269211(21)	2.26893(11)	(*a*)
24	Cr	2.070193(14)	2.07014(17)	(*a*)
25	Mn	1.8964592(58)	1.896457(42)	(*a*)
26	Fe	1.7436170(49)	1.743589(98)	(*a*)
27	Co	1.6083510(42)	1.60836(17)	(*a*)
28	Ni	1.4881401(36)	1.48823(25)	(*a*)
29	Cu	1.3805971(31)	1.38060(16)	(*a*)
30	Zn	1.2833798(40)	1.28338(15)	(*a*)
39	Y	0.7277514(21)	0.727750(23)	(*a*)
40	Zr	0.6889591(31)	0.688946(30)	(*a*)
41	Nb	0.6531341(14)	0.653112(29)	(*a*)
42	Mo	0.61991006(62)	0.619906(64)	(*a*)
45	Rh	0.5339086(69)	0.533951(10)	(*a*)
46	Pd	0.5091212(42)	0.509156(11)	(*a*)
47	Ag	0.4859155(57)	0.4859168(91)	(*a*)
48	Cd	0.4641293(35)	0.464135(12)	(*a*)
49	In	0.4437454(48)	0.443740(11)	(*a*)
50	Sn	0.4245978(29)	0.424590(13)	(*a*)
51	Sb	0.4066324(27)	0.406612(12)	(*a*)
68	Er	0.2156801(75)	0.2156762(50)	(*b*)
82	Pb	0.1408821(74)	0.1408836(11)	(*c*)

References: (*a*) Kraft *et al*. (1996); (*b*) Lum *et al*. (1981); (*c*) Bearden (1960).

Many-body effects are calculated by using relativistic many-body perturbation theory (RMBPT). Since inner vacancy levels are auto-ionizing, one must include shifts in their energy due to the coupling between the discrete levels and Auger decay continuua.

In the following subsections, we describe in more detail the calculation of the different contributions.

4.2.2.9. *Evaluation of the uncorrelated energy with the Dirac–Fock method*

The first step in the calculation, following Indelicato and collaborators (Indelicato & Desclaux, 1990; Indelicato & Lindroth, 1992; Mooney *et al.*, 1992; Lindroth & Indelicato, 1993; Indelicato & Lindroth, 1996) consists in evaluating the best possible energy with relativistic corrections, within the independent electron approximation, for each hole state (here $1s_{\frac{1}{2}}$, $2p_{\frac{1}{2}}$, $2p_{\frac{3}{2}}$, $3p_{\frac{1}{2}}$, $3p_{\frac{3}{2}}$ for K, $L_{\rm II}$, $L_{\rm III}$, $M_{\rm II}$, $M_{\rm III}$, respectively). Such a calculation must provide a suitable starting point for adding all many-body and QED contributions. We have thus chosen the Dirac–Fock method in the implementation of Desclaux (1975, 1993). This method, based on the Dirac equation, allows treatment of arbitrary atoms with arbitrary structure and has been widely used for this kind of calculation. We have used it with full exchange and relaxation (to account for inactive orbital rearrangment due to the hole presence). The electron–electron interaction used in this program contains all magnetic and retardation effects, which is very important to have good results at large Z. The magnetic interaction is treated on an equal footing with the Coulomb interaction, to account for higher-order effects in the wavefunction (which are also useful for evaluating radiative corrections to the electron–electron interaction). All these calculations must be done with proper nuclear charge models to account for finite-nuclear-size corrections to all contributions. For heavy nuclei, nuclear deformations must be accounted for (Blundell, Johnson & Sapirstein, 1990; Indelicato, 1990). For all elements for which experiments have been performed, we used experimental nuclear charge radii. For the others we used a formula from Johnson & Soff (1985), corrected for nuclear deformations for $Z > 90$. Contribution of deformation to the r.m.s. radius (the only parameter of importance to the atomic calculation) is roughly constant (0.11 fm) for $Z > 90$. There is an unknown region, between Bi and Th ($83 < Z < 90$), where deformation effects start to be important, but for which they are not known. When experiments are done for a particular isotope, we calculated separately the energies for each isotope.

As mentioned in the introduction, there are special difficulties involved when dealing with atoms with open outer shells (obviously this is the most common case). Computing all energies E_J for total angular momentum J would be both impossible and useless. The Dirac–Fock method circumvents this difficulty. One can evaluate directly an average energy that corresponds to the barycentre of all E_J with weight $(2J + 1)$. There are still a few cases for which the average calculation cannot converge (when the open shells have identical symmetry). In that case, the outer electrons have been rearranged in an identical fashion for all hole states of the atom, to minimize possible shifts due to this procedure.

4.2.2.10. *Correlation and Auger shifts*

Once the Dirac–Fock energy is obtained, many-body effects beyond Dirac–Fock relaxation must be taken into account. These include relaxation beyond the spherical average, correlation (due to both Coulomb and magnetic interaction), and corrections due to the autoionizing nature of hole states (Auger shift). Since the many-body generalization of the Dirac–Fock method, the so-called MCDF (multiconfiguration Dirac–Fock), is very inefficient for hole states, we turned to RMBPT to evaluate those quantities. These many-body effects contribute very significantly to the final value. Coulomb correlation is mostly constant along the Periodic Table (at the level of a few eV). Magnetic correlations are very strong at high Z. Auger shift is very important for p states. The interested reader will find more details of these complicated calculations in the original references (Indelicato & Lindroth, 1992; Mooney *et al.*, 1992; Lindroth & Indelicato, 1993; Indelicato & Lindroth, 1996). As these calculations are very time consuming, they are performed only for selected Z and interpolated. Since the Auger shifts do not always have a smooth Z dependence, care has been taken to evaluate them at as many different Z's as practical to ensure a good reproduction of irregularities.

4.2.2.11. *QED corrections*

The QED corrections originate in the quantum nature of both the electromagnetic and electron fields. They can be divided in two categories, radiative and non-radiative. The first one includes self-energy and vacuum polarization, which are the main contributions to the Lamb shift in one-electron atoms. These corrections scale as Z^4/n^3 (n being the principal quantum number) and are thus very important for inner shells and high Z. The second category is composed of corrections to the electron–electron interaction that cannot be accounted for by RMBPT or MCDF. These corrections start at the two-photon interaction and include three-body effects. The two-photon, non-radiative QED contribution has been calculated recently only for the ground

Table 4.2.2.4. *Wavelengths of K-emission lines and K-absorption edges in Å; see text for explanation of typefaces*

Numbers in parentheses are standard uncertainties in the least significant figures.

Z	Symbol	A	$K\alpha_2$	$K\alpha_1$	$K\beta_3$	$K\beta_1$	$K\beta_2^{II}$	$K\beta_2^{I}$	K abs. edge
10	Ne		*14.6020(93)*	*14.6006(93)*					*14.2391(26)*
			14.6102(44)	14.6102(44)	14.4522(74)	14.4522(74)			14.30201(15)
11	Na		*11.9013(59)*	*11.8994(59)*					*11.4784(16)*
			11.9103(13)	11.9103(13)	11.5752(30)	11.5752(30)			11.5692(15)
12	Mg		*9.8860(39)*	*9.8840(39)*					*9.4479(10)*
			9.89153(10)	**9.889554(88)**	9.5211(30)	9.5211(30)			9.51234(15)
13	Al		*8.3372(27)*	*8.3349(26)*	*7.9412(49)*				*7.89928(67)*
			8.341831(58)	**8.339514(58)**	7.9601(30)	7.9601(30)			7.948249(74)
14	Si		*7.1269(19)*	*7.1208(19)*	*6.7317(26)*				*6.70091(46)*
			7.12801(14)	**7.125588(78)**	6.7531(15)	6.7531(15)			6.7381(15)
15	P		*6.1587(14)*	*6.1539(14)*	*5.7834(16)*	*5.7914(27)*			*5.75537(33)*
			6.1601(15)	6.1571(15)	5.7961(30)	5.7961(30)			5.7841(15)
16	S		*5.3742(10)*	*5.3701(10)*	*5.0202(12)*	*5.0246(15)*			*4.99591(24)*
			5.374960(89)	**5.372200(78)**		5.03168(30)			5.01858(15)
17	Cl		*4.72993(80)*	*4.72560(77)*	*4.39810(99)*	*4.40038(77)*			*4.37679(18)*
			4.730693(71)	**4.727818(71)**	4.40347(44)	4.40347(44)			4.39717(15)
18	Ar		*4.19448(62)*	*4.19162(60)*	*3.88506(71)*	*3.88486(70)*			*3.86552(14)*
			4.194939(23)	**4.191938(23)**	3.88606(30)	3.88606(30)			3.870958(74)
19	K		*3.74352(50)*	*3.74055(48)*	*3.45189(69)*	*3.45216(58)*			*3.42856(11)*
			3.7443932(68)	**3.7412838(56)**	3.45395(30)	3.45395(30)			3.43655(15)
20	Ca		*3.36223(39)*	*3.35911(38)*	*3.08855(45)*	*3.08827(45)*			*3.061828(87)*
			3.361710(44)	3.358440(44)	3.08975(30)	3.08975(30)			3.07035(15)
21	Sc		*3.03479(33)*	*3.03129(31)*	*2.77919(50)*	*2.77809(49)*			*2.754176(71)*
			3.0344010(63)	3.030854(14)	2.77964(30)	2.77964(30)			2.7620(15)
22	Ti		*2.75272(27)*	*2.74886(26)*	*2.51445(43)*	*2.51262(45)*			*2.490681(59)*
			2.7521950(57)	2.7485471(57)	2.513960(30)	2.513960(30)			2.497377(74)
23	V		*2.50798(23)*	*2.50383(21)*	*2.28567(37)*	*2.28332(40)*			*2.263194(49)*
			2.507430(30)	2.503610(30)	2.284446(30)	2.284446(30)			**2.269211(21)**
24	Cr		*2.29428(19)*	*2.29012(18)*	*2.08702(32)*	*2.08478(35)*			*2.067898(41)*
			2.2936510(30)	**2.2897260(30)**	**2.0848810(40)**	**2.0848810(40)**			**2.070193(14)**
25	Mn		*2.10635(16)*	*2.10210(15)*	*1.91175(28)*	*1.90960(31)*			*1.892275(36)*
			2.1058220(30)	**2.1018540(30)**	**1.9102160(40)**	**1.9102160(40)**			**1.8964592(58)**
26	Fe		*1.94043(14)*	*1.93631(13)*	*1.75784(25)*	*1.75617(27)*			*1.739918(31)*
			1.9399730(30)	**1.9360410(30)**	**1.7566040(40)**	**1.7566040(40)**			**1.7436170(49)**
27	Co		*1.79321(12)*	*1.78919(11)*	*1.62166(22)*	*1.62039(24)*			*1.605127(27)*
			1.7928350(10)	**1.7889960(10)**	**1.6208260(30)**	**1.6208260(30)**			**1.6083510(42)**
28	Ni		*1.66199(10)*	*1.658049(96)*	*1.50059(19)*	*1.49964(21)*			*1.485300(24)*
			1.6617560(10)	**1.6579300(10)**	**1.5001520(30)**	**1.5001520(30)**			**1.4881401(36)**
29	Cu		*1.544324(93)*	*1.540538(85)*	*1.39246(17)*	*1.39201(18)*			*1.379448(23)*
			1.54442740(50)	**1.54059290(50)**	**1.3922340(60)**	**1.3922340(60)**			**1.3805971(31)**
30	Zn		*1.438963(84)*	*1.435151(74)*	*1.29544(17)*	*1.29506(16)*			*1.282346(20)*
			1.439029(12)	1.435184(12)	1.295276(30)	1.295276(30)	1.283739(30)	1.283739(30)	**1.2833798(40)**
31	Ga		*1.343987(72)*	*1.340095(65)*	*1.20821(13)*	*1.20774(14)*	*1.195547(25)*		*1.194711(18)*
			1.3440260(40)	**1.3401270(96)**	1.208390(75)	1.207930(34)	1.196018(30)	1.196018(30)	1.19582(15)
32	Ge		*1.257998(65)*	*1.254054(58)*	*1.12924(13)*	*1.12877(13)*	*1.116387(37)*		*1.115585(16)*
			1.258030(13)	1.254073(13)	1.12938(13)	1.128957(30)	1.116877(30)	1.116877(30)	1.116597(74)
33	As		*1.179921(57)*	*1.175932(52)*	*1.05774(11)*	*1.05724(11)*	*1.044699(56)*	*1.044836(20)*	*1.043925(16)*
			1.179959(17)	**1.17595600(90)**	1.057898(76)	1.057368(33)	1.045016(44)	1.045016(44)	1.04502(15)
34	Se		*1.108801(52)*	*1.104778(47)*	*0.992646(96)*	*0.992152(95)*	*0.979618(57)*	*0.979716(26)*	*0.978818(15)*
			1.108830(31)	**1.104780(12)**	0.992689(79)	0.992189(53)	0.979935(74)	0.979935(74)	0.979755(15)
35	Br		*1.043841(47)*	*1.039785(42)*	*0.933275(87)*	*0.932768(84)*	*0.920344(49)*	*0.920390(28)*	*0.919501(13)*
			1.043836(30)	1.039756(30)	0.933284(74)	0.932804(30)	0.920474(30)	0.920474(30)	0.92041(15)
36	Kr		*0.984347(42)*	*0.980267(38)*	*0.878967(81)*	*0.878495(75)*	*0.866209(36)*	*0.866169(35)*	*0.865324(12)*
			0.9843590(44)	**0.9802670(40)**	**0.8790110(70)**	**0.8785220(50)**	0.86611(15)	0.86611(15)	0.865533(15)
37	Rb		*0.929713(39)*	*0.925597(35)*	*0.829174(71)*	*0.828681(67)*	*0.816459(33)*	*0.816408(33)*	*0.815270(12)*
			0.929704(15)	0.925567(13)	0.829222(44)	0.828692(30)	0.816462(44)	0.816462(44)	0.815552(74)
38	Sr		*0.879444(36)*	*0.875298(32)*	*0.783413(63)*	*0.782911(58)*	*0.770774(33)*	*0.770718(20)*	*0.769359(11)*
			0.879443(15)	0.875273(15)	0.783462(44)	0.782932(30)	0.770822(44)	0.770822(44)	0.769742(74)
39	Y		*0.833059(32)*	*0.828875(29)*	*0.741232(58)*	*0.740716(53)*	*0.728801(27)*	*0.728663(21)*	*0.727270(10)*
			0.833063(15)	0.828852(15)	0.741271(44)	0.740731(30)	0.728651(59)	0.728651(59)	**0.7277514(21)**
40	Zr		*0.790181(30)*	*0.785960(27)*	*0.702296(53)*	*0.701766(48)*	*0.690079(28)*	*0.689895(21)*	*0.6884893(99)*
			0.7901790(25)	**0.7859579(27)**	**0.7023554(30)**	**0.7018008(30)**	0.689940(59)	0.689940(59)	**0.6889591(31)**
41	Nb		*0.750448(28)*	*0.746189(25)*	*0.666266(49)*	*0.665721(44)*	*0.654328(31)*	*0.654078(22)*	*0.6528690(93)*
			0.750451(15)	0.746211(15)	0.666350(44)	0.665770(30)	0.654170(59)	0.654170(59)	**0.6531341(14)**
42	Mo		*0.713612(25)*	*0.709328(22)*	*0.632900(44)*	*0.632345(38)*	*0.621162(35)*	*0.620941(21)*	*0.6196481(87)*
			0.713607(12)	**0.70931715(41)**	0.632887(13)	0.632303(13)	0.620999(30)	0.620999(30)	**0.61991006(62)**

Table 4.2.2.4. *Wavelengths of K-emission lines and K-absorption edges in Å (cont.)*

Z	Symbol	A	$K\alpha_2$	$K\alpha_1$	$K\beta_3$	$K\beta_1$	$K\beta_2^{II}$	$K\beta_2^{I}$	K abs. edge
43	Tc		*0.679318(24)*	*0.675017(21)*	*0.601881(40)*	*0.601318(35)*	*0.590423(40)*	*0.590231(22)*	*0.5889852(84)*
			0.679330(44)	0.675030(44)	0.601889(59)	0.601309(59)	0.590249(74)	0.590249(74)	0.589069(15)
44	Ru		*0.647415(22)*	*0.643088(20)*	*0.573053(37)*	*0.572478(32)*	*0.561748(44)*	*0.561587(22)*	*0.5603122(81)*
			0.6474205(61)	0.6430994(61)	0.5730816(42)	0.5724966(42)	0.561668(44)	0.561668(44)	0.560518(15)
45	Rh		*0.617652(21)*	*0.613305(18)*	*0.546191(34)*	*0.545606(29)*	*0.535110(48)*	*0.534977(22)*	*0.5337192(74)*
			0.6176458(61)	0.6132937(61)	0.5462139(42)	0.5456189(42)	0.535038(30)	0.535038(30)	**0.5339086(69)**
46	Pd		*0.589822(20)*	*0.585459(18)*	*0.521117(29)*	*0.520514(27)*	*0.510283(46)*	*0.510177(51)*	*0.5090158(75)*
			0.5898351(60)	0.5854639(46)	0.5211363(41)	0.5205333(41)	0.5102357(59)	0.5102357(59)	0.5091212(42)
47	Ag		*0.563804(18)*	*0.559420(17)*	*0.497673(29)*	*0.497069(25)*	*0.487060(55)*	*0.487019(38)*	*0.4857609(74)*
			0.5638131(26)	**0.55942178(76)**	0.4976977(60)	0.4970817(60)	0.4870393(59)	0.4870393(59)	**0.4859155(57)**
48	Cd		*0.539426(18)*	*0.535020(15)*	*0.475739(27)*	*0.475124(23)*	*0.465335(62)*	*0.465346(28)*	*0.4640026(71)*
			0.5394358(46)	0.5350147(46)	0.4757401(71)	0.4751181(71)	0.465335(10)	0.465335(10)	**0.4641293(35)**
49	In		*0.516551(17)*	*0.512124(15)*	*0.455178(25)*	*0.454552(22)*	*0.445014(58)*	*0.445011(27)*	*0.4435977(70)*
			0.5165572(60)	0.5121251(46)	0.4551966(41)	0.4545616(41)	0.445007(15)	0.445007(15)	**0.4437454(48)**
50	Sn		*0.495060(16)*	*0.490612(14)*	*0.435878(24)*	*0.435241(20)*	*0.426120(12)*	*0.425928(26)*	*0.4244611(68)*
			0.4950646(46)	0.4906115(46)	0.4358821(51)	0.4352421(51)	0.425921(12)	0.425921(12)	**0.4245978(29)**
51	Sb		*0.474840(15)*	*0.470373(13)*	*0.417736(22)*	*0.417089(19)*	*0.408017(57)*	*0.408004(25)*	*0.4064886(65)*
			0.4748391(45)	0.4703700(45)	0.4177477(41)	0.4170966(31)	0.4079791(74)	0.4079791(74)	**0.4066324(27)**
52	Te		*0.455795(14)*	*0.451310(13)*	*0.400664(21)*	*0.400008(18)*	*0.391161(56)*	*0.391135(27)*	*0.3895899(64)*
			0.4557908(44)	0.4513018(44)	0.4006650(59)	0.4000010(44)	0.3911079(89)	0.3911079(89)	0.389746(15)
53	I		*0.437834(13)*	*0.433330(12)*	*0.384576(20)*	*0.383910(17)*	*0.375286(54)*	*0.375234(29)*	*0.3736775(61)*
			0.437836(10)	0.4333245(74)	0.3845698(59)	0.3839108(59)	0.375236(30)	0.375236(30)	0.373816(15)
54	Xe		*0.420879(42)*	*0.416358(40)*	*0.369407(40)*	*0.368730(38)*	*0.360326(72)*	*0.36034(12)*	*0.358683(27)*
			0.42088103(71)	**0.4163508(14)**	**0.3694051(13)**	**0.3687346(13)**	0.360265(44)	0.360265(44)	0.35841(74)
55	Cs		*0.404848(13)*	*0.400310(11)*	*0.355067(17)*	*0.354385(16)*	*0.346197(49)*	*0.346102(37)*	*0.3444778(59)*
			0.4048411(59)	0.4002960(59)	0.3550553(59)	0.354369(10)	0.346115(30)	0.346115(30)	0.344515(15)
56	Ba		*0.389684(12)*	*0.385129(11)*	*0.341517(16)*	*0.340826(15)*	*0.33285(14)*	*0.332728(12)*	*0.3310639(56)*
			0.38968378(74)	**0.38512464(84)**	**0.3415228(11)**	**0.34082708(75)**	0.332775(15)	0.332775(15)	0.331045(15)
57	La		*0.375320(11)*	*0.370748(10)*	*0.328692(16)*	*0.327993(14)*	*0.32023(13)*	*0.320101(11)*	*0.3184025(55)*
			0.3753186(30)	0.3707426(30)	0.3286909(59)	0.3279879(44)	0.320122(10)	0.320122(10)	0.318445(74)
58	Ce		*0.361685(11)*	*0.3570964(97)*	*0.316507(15)*	*0.315795(14)*	*0.30827(12)*	*0.308131(10)*	*0.3065382(54)*
			0.3616884(30)	0.3570974(30)	0.3165248(59)	0.3158207(30)	0.308165(15)	0.308165(15)	0.306485(74)
59	Pr		*0.348755(10)*	*0.3441494(94)*	*0.304970(14)*	*0.304249(13)*	*0.29694(11)*	*0.2967952(99)*	*0.2952418(53)*
			0.3487542(30)	0.3441452(30)	0.3049796(74)	0.3042656(59)	0.296794(30)	0.296794(30)	0.295184(74)
60	Nd		*0.336473(10)*	*0.3318514(91)*	*0.294021(13)*	*0.293290(13)*	*0.28619(10)*	*0.2860408(94)*	*0.2845288(52)*
			0.33647921(73)	**0.33185689(62)**	0.2940366(40)	0.2933086(40)	0.28610(15)	0.28610(15)	0.284534(74)
61	Pm		*0.3247982(98)*	*0.3201607(88)*	*0.283620(13)*	*0.282880(12)*	*0.275992(98)*	*0.2758335(91)*	*0.2743634(53)*
			0.3248079(59)	0.3201648(59)	0.283634(59)	0.282904(44)	0.27590(15)	0.27590(15)	0.274314(74)
62	Sm		*0.3136913(94)*	*0.3090384(84)*	*0.273732(12)*	*0.272984(12)*	*0.266459(91)*	*0.2661277(87)*	*0.2647027(51)*
			0.31369830(79)	**0.30904506(46)**	0.273764(30)	0.273014(30)	0.26620(15)	0.26620(15)	0.264644(74)
63	Eu		*0.3031139(91)*	*0.2984457(81)*	*0.264322(12)*	*0.263567(11)*	*0.257069(85)*	*0.2569028(81)*	*0.2555123(51)*
			0.3031225(30)	0.2984505(30)	0.2643360(74)	0.2635810(74)	0.256927(12)	0.256927(12)	0.255534(15)
64	Gd		*0.2930400(89)*	*0.2883568(79)*	*0.255371(11)*	*0.254610(11)*	*0.248289(23)*	*0.2481186(76)*	*0.2467265(48)*
			0.2930424(30)	0.2883573(30)	0.255344(30)	0.254604(30)	0.248164(44)	0.248164(44)	0.246814(15)
65	Tb		*0.2834212(86)*	*0.2787234(76)*	*0.246818(11)*	*0.246054(11)*	*0.239916(21)*	*0.2397496(75)*	*0.2384335(49)*
			0.2834273(30)	0.2787242(30)	0.246834(30)	0.246084(30)	0.23970(30)	0.23970(30)	0.238414(15)
66	Dy		*0.2742462(84)*	*0.2695341(74)*	*0.238671(10)*	*0.237902(10)*	*0.231955(12)*	*0.2318190(53)*	*0.2304867(46)*
			0.2742511(30)	0.2695370(30)	0.238624(30)	0.237884(30)	0.23170(30)	0.23170(30)	0.230483(15)
67	Ho		*0.2654851(81)*	*0.2607589(72)*	*0.230896(10)*	*0.230122(10)*	*0.224320(18)*	*0.2241536(66)*	*0.2229099(45)*
			0.26549088(84)	0.2607608(42)	0.230834(30)	0.230124(30)	0.22410(30)	0.22410(30)	0.222913(15)
68	Er		*0.2571059(79)*	*0.2523659(71)*	*0.2234662(97)*	*0.2226875(98)*	*0.217046(16)*	*0.2168806(64)*	*0.2156719(45)*
			0.2571133(11)	**0.25237359(62)**	**0.2234766(14)**	**0.22269866(72)**	0.21670(30)	0.21670(30)	**0.2156801(75)**
69	Tm		*0.2490952(77)*	*0.2443415(68)*	*0.2163665(94)*	*0.2155833(95)*	*0.210099(15)*	*0.2099331(62)*	*0.2087587(44)*
			0.24910095(61)	0.24434486(44)	0.216366(30)	0.21559182(57)	0.20980(30)	0.20980(30)	0.208803(74)
70	Yb		*0.2414274(75)*	*0.2366603(67)*	*0.2095741(93)*	*0.2087863(95)*	*0.203456(14)*	*0.2032912(59)*	*0.2021481(43)*
			0.2414276(30)	0.2366586(30)	0.20960(15)	0.208843(30)	0.20330(30)	0.20330(30)	0.202243(74)
71	Lu		*0.2340857(73)*	*0.2293053(65)*	*0.2030802(88)*	*0.2022872(90)*	*0.197101(13)*	*0.1969329(58)*	*0.1957973(42)*
			0.2340845(30)	0.2293014(30)	0.203093(59)	0.202313(44)	0.19690(30)	0.19690(30)	0.195853(74)
72	Hf		*0.2270507(72)*	*0.2222572(64)*	*0.1968603(86)*	*0.1960622(88)*	*0.191017(13)*	*0.1908468(56)*	*0.1897176(42)*
			0.2270274(44)	0.2222303(44)	0.196863(59)	0.196073(44)	0.19080(30)	0.19080(30)	0.189823(74)
73	Ta		*0.2203039(70)*	*0.2154977(63)*	*0.1908986(83)*	*0.1900954(86)*	*0.185143(12)*	*0.1849702(54)*	*0.1838657(41)*
			0.2203083(59)	0.2155002(59)	0.1908929(30)	0.1900919(59)	0.185191(13)	0.185014(12)	0.183943(15)
74	W		*0.2138327(69)*	*0.2090134(61)*	*0.1851834(81)*	*0.1843751(83)*	*0.179595(12)*	*0.1794215(52)*	*0.1783098(41)*
			0.21383304(50)	**0.20901314(18)**	**0.18518317(70)**	**0.1843768(30)**	0.179603(15)	0.179424(10)	0.178373(15)
75	Re		*0.2076150(67)*	*0.2027835(60)*	*0.1796955(79)*	*0.1788824(81)*	*0.174234(11)*	*0.1740571(51)*	*0.1729509(40)*
			0.2076141(15)	0.2027840(30)	0.1796997(44)	0.1788827(44)	0.174253(15)	0.1740566(89)	0.173023(15)

Table 4.2.2.4. *Wavelengths of K-emission lines and K-absorption edges in Å (cont.)*

Z	Symbol	A	$K\alpha_2$	$K\alpha_1$	$K\beta_3$	$K\beta_1$	$K\beta_2^{II}$	$K\beta_2^{I}$	K abs. edge
76	Os		*0.2016443(66)*	*0.1968007(59)*	*0.1744279(77)*	*0.1736101(79)*	*0.169085(11)*	*0.1689066(50)*	*0.1678092(40)*
			0.2016420(30)	0.1967970(30)	0.1744336(44)	0.1736136(44)	0.169103(15)	0.1689085(89)	0.167873(15)
77	Ir		*0.1959045(65)*	*0.1910492(57)*	*0.1693667(75)*	*0.1685444(77)*	*0.164150(11)*	*0.1639697(51)*	*0.1628853(39)*
			0.1959069(30)	0.1910499(30)	0.1693695(30)	0.1685445(30)	0.164152(15)	0.163958(10)	0.162922(15)
78	Pt		*0.1903859(61)*	*0.1855187(55)*	*0.1645026(72)*	*0.1636756(74)*	*0.1593872(99)*	*0.1592048(46)*	*0.1581346(38)*
			0.1903839(59)	0.1855138(59)	0.1645035(44)	0.1636775(44)	0.159392(15)	0.159202(15)	0.158182(15)
79	Au		*0.1850702(64)*	*0.1801914(57)*	*0.1598202(73)*	*0.1589887(75)*	*0.1548206(99)*	*0.1546363(48)*	*0.1535699(40)*
			0.18507664(61)	**0.18019780(47)**	**0.1598249(13)**	**0.15899527(77)**	0.154832(30)	0.154620(13)	0.1535953(74)
80	Hg		*0.1799628(61)*	*0.1750720(54)*	*0.1553217(69)*	*0.1544857(72)*	*0.1504204(94)*	*0.1502334(46)*	*0.1491786(38)*
			0.1799607(44)	0.1750706(44)	0.1553233(44)	0.1544893(44)	0.150402(30)	0.150202(30)	0.149182(15)
81	Tl		*0.1750380(60)*	*0.1701355(53)*	*0.1509866(68)*	*0.1501462(70)*	*0.1461874(92)*	*0.1459989(77)*	*0.1449460(37)*
			0.1750386(30)	0.1701386(30)	0.1509823(89)	0.1501443(74)	0.146142(15)	0.145952(15)	0.144952(15)
82	Pb		*0.1702924(59)*	*0.1653781(53)*	*0.1468107(67)*	*0.1459663(68)*	*0.1421118(88)*	*0.1419201(75)*	*0.1408707(37)*
			0.17029527(56)	**0.16537816(38)**	**0.1468129(10)**	**0.14596836(58)**	0.142122(30)	0.141912(15)	0.1408821(74)
83	Bi	209	*0.1657170(58)*	*0.1607911(52)*	*0.1427865(65)*	*0.1419372(66)*	*0.1381841(87)*	*0.1379910(72)*	*0.1369439(37)*
			0.1657183(20)	0.1607903(46)	0.142780(11)	0.1419492(54)	0.138172(15)	0.137972(15)	0.136942(15)
84	Po	209	*0.1613031(58)*	*0.1563656(51)*	*0.1389056(63)*	*0.1380520(65)*	*0.1343966(85)*	*0.1342012(69)*	*0.1331589(36)*
			0.161302(15)	0.156362(15)	0.138922(30)	0.138072(30)	0.134382(30)	0.134182(30)	
85	At	210	*0.1570444(56)*	*0.1520953(50)*	*0.1351623(62)*	*0.1343044(63)*	*0.1307448(83)*	*0.1305470(67)*	*0.1295098(36)*
			0.157052(30)	0.152102(30)	0.135172(59)	0.134322(59)	0.130722(59)	0.130522(59)	
86	Rn	222	*0.1529334(56)*	*0.1479727(49)*	*0.1315499(61)*	*0.1306882(61)*	*0.1272218(79)*	*0.1270211(66)*	*0.1259898(35)*
			0.152942(44)	0.147982(44)	0.131552(74)	0.130692(74)	0.127192(74)	0.126982(74)	
87	Fr	223	*0.1489599(56)*	*0.1439878(50)*	*0.1280599(60)*	*0.1271937(61)*	*0.1238183(79)*	*0.1236157(63)*	*0.1225852(36)*
			0.148962(44)	0.143992(44)	0.128072(74)	0.127192(74)	0.123792(74)	0.123582(74)	
88	Ra	226	*0.1451209(54)*	*0.1401373(48)*	*0.1246890(58)*	*0.1238185(59)*	*0.1205312(77)*	*0.1203271(60)*	*0.1192985(35)*
			0.145119(20)	0.140132(19)	0.124689(15)	0.123815(15)	0.120535(14)	0.120320(14)	
89	Ac	227	*0.1414083(54)*	*0.1364131(47)*	*0.1214301(57)*	*0.1205554(58)*	*0.1173552(73)*	*0.1171477(59)*	*0.1161246(34)*
			0.141412(30)	0.136419(12)	0.121432(30)	0.120552(30)	0.117322(30)	0.117112(30)	
90	Th	232	*0.1378266(53)*	*0.1328194(47)*	*0.1182861(56)*	*0.1174071(56)*	*0.1142910(71)*	*0.1140810(57)*	*0.1130642(34)*
			0.13782600(31)	**0.13282021(36)**	**0.11828686(78)**	**0.11740759(59)**	0.114262(15)	0.114042(13)	0.113072(15)
91	Pa	231	*0.1343514(52)*	*0.1293324(46)*	*0.1152364(55)*	*0.1143530(55)*	*0.1113088(69)*	*0.1110964(56)*	*0.1101087(34)*
			0.1343516(29)	0.1293302(27)	0.1152427(21)	0.1143583(21)	0.111292(30)	0.111072(30)	
92	U	238	*0.1309879(52)*	*0.1259572(46)*	*0.1122860(53)*	*0.1113979(54)*	*0.1084449(67)*	*0.1082301(54)*	*0.1072452(33)*
			0.13099111(78)	**0.12595977(36)**	**0.11228858(66)**	**0.11140132(65)**	0.108372(15)	0.108182(15)	0.107232(15)
93	Np	237	*0.1277298(51)*	*0.1226871(45)*	*0.1094299(52)*	*0.1085378(53)*	*0.1056621(66)*	*0.1054450(53)*	*0.1044744(33)*
			0.1277287(39)	0.1226882(36)	0.1094230(39)	0.1085265(28)	0.105670(31)	0.105457(31)	0.1044605(62)
94	Pu	244	*0.1245763(50)*	*0.1195212(45)*	*0.1066627(51)*	*0.1057661(52)*	*0.1029688(64)*	*0.1027494(52)*	*0.1017982(33)*
			0.1245705(25)	0.1195140(23)	0.1066611(18)	0.1057595(18)	0.1029724(26)	0.1027429(26)	
95	Am	243	*0.1215172(50)*	*0.1164501(45)*	*0.1039811(51)*	*0.1030805(51)*	*0.1003579(63)*	*0.1001364(51)*	*0.0991999(33)*
			0.1215158(24)	0.1164463(33)	0.1039794(17)	0.1030803(17)	0.1003537(24)	0.1001357(24)	
96	Cm	248	*0.1185536(49)*	*0.1134742(44)*	*0.1013837(50)*	*0.1004790(50)*	*0.0978295(63)*	*0.0976059(50)*	*0.0966801(33)*
			0.1185427(23)	0.1134635(21)	0.1013753(17)	0.1004708(16)	0.0978355(23)	0.0975952(15)	
97	Bk	249	*0.1156777(49)*	*0.1105860(43)*	*0.0988636(48)*	*0.0979546(49)*	*0.0953724(61)*	*0.0951469(49)*	*0.0942405(32)*
			0.1156630(54)	0.1105745(49)	0.0988598(55)	0.0979514(54)		0.0942501(50)	
98	Cf	250	*0.1128873(48)*	*0.1077832(43)*	*0.0964130(47)*	*0.0955000(48)*	*0.0929867(61)*	*0.0927593(48)*	*0.0918695(32)*
			0.1128799(82)	0.1077793(75)	0.0963915(83)	0.0954860(90)	0.0929715(82)	0.0927508(84)	0.091862(10)
99	Es	251	*0.1101788(47)*	*0.1050620(43)*	*0.0940403(46)*	*0.0931231(47)*	*0.0906838(60)*	*0.0904543(47)*	*0.0895840(32)*
			0.1102072(98)	0.1050554(89)	0.094036(14)	0.093090(14)			0.0895878(97)
100	Fm	254	*0.1075497(47)*	*0.1024201(42)*	*0.0917379(45)*	*0.0908165(46)*	*0.0884443(59)*	*0.0882127(45)*	*0.0873575(32)*
			0.107514(14)	0.102386(13)	0.091715(10)	0.0907943(98)	0.0884212(100)	0.0881872(99)	0.0873356(80)

state of two-electron ions (Blundell, Mohr, Johnson & Sapirstein, 1993; Lindgren, Persson, Salomonson & Labzowsky, 1995) and cannot be evaluated in practice for atoms with more than two or three electrons.

The radiative corrections split up into two contributions. The first contribution is composed of one-electron radiative corrections (self-energy and vacuum polarization). For the self-energy and $Z > 10$, one must use all-order calculations (Mohr, 1974*a*,*b*, 1975, 1982, 1992; Mohr & Soff, 1993). Vacuum polarization can be evaluated at the Uehling (1935) and Wichmann & Kroll (1956) level. Higher-order effects are much smaller than for the self-energy (Soff & Mohr, 1988) and have been neglected. The second contribution is composed of radiative corrections to the electron–electron interaction, and scales as Z^3/n^3. *Ab initio* calculations have been performed only for few-electron ions (Indelicato & Mohr, 1990, 1991). Here we use the Welton approximation which has been shown to reproduce very closely *ab initio* results in all examples that have been calculated (Indelicato, Gorceix & Desclaux 1987; Indelicato & Desclaux 1990; Kim, Baik, Indelicato & Desclaux, 1991; Blundell, 1993*a*,*b*).

Table 4.2.2.5. *Wavelengths of L-emission lines and L-absorption edges in Å; see text for explanation of typefaces*

Numbers in parentheses are standard uncertainties in the least significant figures.

Z	Symbol	A	$L\alpha_2$	$L\alpha_1$	$L\beta_1$	$L\beta_2$	$L_{\rm I}$ abs. edge	$L_{\rm II}$ abs. edge	$L_{\rm III}$ abs. edge
20	Ca						*28.275(32)*	*35.384(40)*	*35.7704(68)*
			36.331(30)	36.331(30)	35.941(30)			35.131(15)	35.491(15)
21	Sc		*30.947(46)*		*30.587(47)*		*24.896(15)*	*30.718(17)*	*31.109(36)*
			31.350(44)	31.350(44)	31.020(30)				
22	Ti		*27.215(37)*		*26.843(37)*		*22.099(24)*	*26.953(14)*	*27.3105(36)*
			27.420(30)	27.420(30)	27.050(30)			27.290(15)	27.290(15)
23	V		*24.143(30)*		*23.764(30)*		*19.779(19)*	*23.8561(89)*	*24.206(10)*
			24.250(44)	24.250(44)	23.880(59)				
24	Cr		*21.640(24)*	*21.490(11)*	*21.276(24)*		*17.804(15)*	*21.246(18)*	*21.5867(49)*
			21.640(44)	21.640(44)	21.270(15)		16.70(15)	17.90(15)	20.70(15)
25	Mn		*19.390(20)*	*19.359(21)*	*19.036(20)*		*16.113(19)*	*19.0781(57)*	*19.4063(43)*
			19.450(15)	19.450(15)	19.110(30)				
26	Fe		*17.525(17)*	*17.503(17)*	*17.194(17)*		*14.611(34)*	*17.2248(92)*	*17.5402(35)*
			17.590(30)	17.590(30)	17.260(15)			17.2023(74)	17.5253(74)
27	Co		*15.922(14)*	*15.905(15)*	*15.610(14)*		*13.4000(86)*	*15.627(14)*	*15.9290(44)*
			15.9722(89)	15.9722(89)	15.666(12)			15.6182(74)	15.9152(74)
28	Ni		*14.532(12)*	*14.520(12)*	*14.236(12)*		*12.295(13)*	*14.251(23)*	*14.5396(57)*
			14.5612(44)	14.5612(44)	14.2712(89)			14.2422(74)	14.5252(74)
29	Cu		*13.341(10)*	*13.336(11)*	*13.063(10)*		*11.292(16)*	*13.016(14)*	*13.2934(64)*
			13.3362(44)	13.3362(44)	13.0532(44)			13.0142(15)	13.2882(15)
30	Zn		*12.2529(90)*	*12.2489(90)*	*11.9819(93)*		*10.361(12)*	*11.8652(66)*	*12.134(14)*
			12.2542(44)	12.2542(44)	11.9832(44)		13.060(15)	11.8622(15)	12.1312(15)
31	Ga		*11.2916(77)*	*11.2858(78)*	*11.0226(78)*		*9.518(11)*	*10.8414(29)*	*11.1040(29)*
			11.2922(15)	11.2922(15)	11.0232(30)		9.5171(74)	10.8282(74)	11.1002(15)
32	Ge		*10.4371(68)*	*10.4306(68)*	*10.1717(69)*		*8.775(12)*	*9.9340(27)*	*10.1849(46)*
			10.4363(12)	10.4363(12)	10.1752(15)		8.7731(15)	9.9241(15)	10.1872(15)
33	As		*9.6744(60)*	*9.6680(60)*	*9.4126(59)*		*8.092(13)*	*9.1182(17)*	*9.3649(29)*
			9.6710(12)	9.6710(12)	9.4142(12)		8.1071(15)	9.1251(15)	9.3671(15)
34	Se		*8.9914(52)*	*8.9852(52)*	*8.7335(52)*		*7.498(13)*	*8.4105(58)*	*8.64459(77)*
			8.99013(74)	8.99013(74)	8.73593(74)		7.5031(15)	8.4071(15)	8.6461(15)
35	Br		*8.3776(46)*	*8.3715(46)*	*8.1233(46)*		*6.958(14)*	*7.7669(35)*	*7.9991(30)*
			8.37473(74)	8.37473(74)	8.12522(74)		6.9591(74)	7.7531(74)	7.9841(74)
36	Kr		*7.8242(41)*	*7.8180(41)*	*7.5736(40)*		*6.4561(41)*	*7.1630(21)*	*7.3841(17)*
			7.82032(13)	**7.82032(13)**	**7.574441(98)**		6.470(15)	7.1681(15)	7.3921(15)
37	Rb		*7.3226(37)*	*7.3164(36)*	*7.0749(36)*		*6.0010(11)*	*6.6449(59)*	*6.8643(67)*
			7.32521(44)	7.31841(30)	7.07601(44)		6.0081(74)	6.6441(15)	6.8621(15)
38	Sr		*6.8674(33)*	*6.8610(32)*	*6.6224(33)*		*5.5945(16)*	*6.17624(70)*	*6.38937(84)*
			6.86980(44)	6.86290(30)	6.62400(44)		5.5921(74)	6.1731(15)	6.3871(15)
39	Y		*6.4539(30)*	*6.4466(29)*	*6.2110(29)*		*5.22968(53)*	*5.75742(82)*	*5.9658(15)*
			6.45590(44)	6.44890(30)	6.21209(44)		5.2171(74)	5.7561(15)	5.9621(15)
40	Zr		*6.0766(27)*	*6.0684(26)*	*5.8357(26)*		*4.89881(41)*	*5.3773(15)*	*5.5816(15)*
			6.0766(27)	**6.070250(79)**	**5.836214(76)**	5.58638(44)*	4.8791(74)	5.3781(15)	5.5791(15)
41	Nb		*5.7326(24)*	*5.7226(23)*	*5.4931(23)*		*4.59975(43)*	*5.03480(63)*	*5.23529(98)*
			5.73199(44)	5.72439(30)	5.49238(44)	5.23798(44)*	4.5751(74)	5.0311(15)	5.2301(15)
42	Mo		*5.4151(22)*	*5.4054(21)*	*5.1778(21)*	*4.91857(74)*	*4.32423(40)*	*4.72145(60)*	*4.9179(31)*
			5.41445(12)	5.40663(12)	5.17716(12)	4.92327(30)*	4.3041(74)	4.7191(15)	4.9131(15)
43	Tc		*5.1228(20)*	*5.1139(19)*	*4.8880(19)*	*4.6341(13)*		*4.4368(13)*	*4.62991(94)*
				5.11488(44)	4.8874(12)		4.0581(74)	4.4361(15)	4.6301(15)
44	Ru		*4.8541(18)*	*4.8449(17)*	*4.6210(17)*	*4.3681(13)*	*3.8443(16)*	*4.17814(78)*	*4.36776(32)*
			4.85388(10)	4.845823(74)	4.620649(44)	4.37187(30)*	3.8351(74)	4.1801(15)	4.3691(15)
45	Rh		*4.6055(16)*	*4.5966(16)*	*4.3744(16)*	*4.1277(12)*	*3.6334(17)*	*3.94053(55)*	*4.12730(50)*
			4.60552(13)	4.59750(13)	4.374206(59)	4.13106(30)*	3.6291(74)	3.94256(74)	4.12996(74)
46	Pd		*4.3753(15)*	*4.3672(15)*	*4.1461(14)*	*3.9088(10)*	*3.43948(61)*	*3.72251(52)*	*3.90655(62)*
			4.37595(10)	4.367736(74)	4.146282(74)	3.908929(59)*	3.4371(15)	3.72286(15)	3.90746(15)
47	Ag		*4.1623(14)*	*4.1541(13)*	*3.9347(13)*	*3.7034(10)*	*3.25639(29)*	*3.51704(26)*	*3.69817(53)*
			4.163002(74)	4.154492(44)	3.934789(44)	3.703406(44)*	3.25645(15)	3.51645(15)	3.69996(15)
48	Cd		*3.9644(13)*	*3.9560(12)*	*3.7382(12)*	*3.51355(97)*	*3.08443(17)*	*3.32528(29)*	*3.50348(45)*
			3.965020(89)	3.956409(59)	3.738286(59)	3.514133(59)*	3.08495(15)	3.32575(15)	3.50475(15)
49	In		*3.7802(12)*	*3.7716(11)*	*3.5553(11)*	*3.33796(83)*	*2.92533(19)*	*3.14784(47)*	*3.32322(42)*
			3.780787(89)	3.771977(59)	3.555363(59)	3.338430(44)*	2.92604(15)	3.14735(15)	3.32375(15)
50	Sn		*3.6084(11)*	*3.5997(10)*	*3.38472(100)*	*3.17475(77)*	*2.776792(71)*	*2.98309(56)*	*3.15521(70)*
			3.606964(59)	3.599994(44)	3.384921(44)	3.175098(44)*	2.77694(15)	2.98234(15)	3.15575(15)

* These values are for the unresolved $L\beta_2$ and $L\beta_{15}$ emission lines.

Table 4.2.2.5. *Wavelengths of L-emission lines and L-absorption edges in Å (cont.)*

Z	Symbol	A	$L\alpha_2$	$L\alpha_1$	$L\beta_1$	$L\beta_2$	$L_{\rm I}$ abs. edge	$L_{\rm II}$ abs. edge	$L_{\rm III}$ abs. edge
51	Sb		*3.44794(99)*	*3.43913(93)*	*3.22551(92)*	*3.02325(67)*	*2.638437(69)*	*2.82990(51)*	*2.99986(66)*
			3.448452(89)	3.439462(59)	3.225718(59)	3.023395(44)*	2.63884(15)	2.82944(74)	3.00035(15)
52	Te		*3.29788(92)*	*3.28894(86)*	*3.07663(85)*	*2.88209(61)*	*2.50998(50)*	*2.687685(87)*	*2.85523(35)*
			3.29851(13)	3.289249(89)	3.076816(89)	2.88221(12)*	2.50994(15)	2.68794(15)	2.85554(15)
53	I		*3.15734(85)*	*3.14828(81)*	*2.93720(78)*	*2.75031(54)*	*2.38965(37)*	*2.55532(31)*	*2.72067(32)*
			3.157957(89)	3.148647(89)	2.937484(89)	2.75057(12)*	2.38804(74)	2.55424(74)	2.71964(74)
54	Xe		*3.02568(78)*	*3.01640(76)*	*2.80659(69)*	*2.62740(47)*	*2.273869(70)*	*2.427862(95)*	*2.590303(89)*
			3.025940(22)	**3.016582(15)**	**2.806553(19)**		2.27373(15)	2.42924(15)	2.59264(15)
55	Cs		*2.90167(73)*	*2.89237(69)*	*2.68362(66)*	*2.51216(47)*	*2.1676(29)*	*2.3135(17)*	*2.47326(16)*
			2.90204(30)	2.89244(30)	2.68374(30)	2.51184(30)*	2.16733(74)	2.31393(15)	2.47404(15)
56	Ba		*2.78522(68)*	*2.77580(64)*	*2.56812(61)*	*2.40421(26)*	*2.0697(15)*	*2.20482(12)*	*2.363082(97)*
			2.785572(74)	2.775992(74)	2.568249(74)	2.404386(89)*	2.06783(74)	2.20483(15)	2.36294(15)
57	La		*2.67563(64)*	*2.66607(60)*	*2.45941(57)*	*2.30307(24)*	*1.97705(28)*	*2.10317(10)*	*2.25958(20)*
			2.675383(60)	2.665740(74)	2.458947(74)	2.303312(98)*	1.97803(74)	2.10533(74)	2.2610(15)
58	Ce		*2.57122(59)*	*2.56108(56)*	*2.35598(53)*	*2.20843(21)*	*1.89320(71)*	*2.01084(14)*	*2.16586(39)*
			2.57059(18)	2.56163(17)	2.35580(18)	2.20900(17)*	1.89343(74)	2.01243(74)	2.1660(15)
59	Pr		*2.47329(55)*	*2.46280(52)*	*2.25890(49)*	*2.11936(20)*	*1.81477(33)*	*1.92607(36)*	*2.07945(22)*
			2.47294(44)	2.46304(30)	2.25883(44)	2.11943(59)*	1.81413(74)	1.92553(74)	2.07913(74)
60	Nd		*2.38081(51)*	*2.36999(48)*	*2.16724(45)*	*2.03554(18)*	*1.73904(18)*	*1.84373(16)*	*1.99616(19)*
			2.38079(52)	**2.370526(16)**	**2.167008(19)**	2.035448(88)*	1.73903(15)	1.84403(15)	1.99673(15)
61	Pm		*2.29340(48)*	*2.28227(45)*	*2.08060(42)*	*1.95675(18)*			
			2.29263(59)	2.28223(44)	2.07973(59)	1.95593(89)*	1.66743(74)	1.76763(74)	1.91913(15)
62	Sm		*2.21054(48)*	*2.19926(42)*	*1.99850(42)*	*1.88225(17)*	*1.60201(12)*	*1.69495(13)*	*1.84534(42)*
			2.210430(24)	**2.199873(13)**	**1.998432(30)**	1.882206(41)*	1.60022(15)	1.69533(15)	1.84573(15)
63	Eu		*2.13214(42)*	*2.12081(40)*	*1.92080(37)*	*1.81237(16)*	*1.54065(17)*	*1.62830(21)*	*1.77767(16)*
			2.13156(17)	2.120673(95)	1.92053(17)	1.81215(17)*	1.53812(15)	1.62712(15)	1.77613(15)
64	Gd		*2.05817(40)*	*2.04670(37)*	*1.84744(34)*	*1.74582(14)*	*1.47922(25)*	*1.56264(23)*	*1.71092(21)*
			2.05783(30)	2.04683(30)	1.84683(30)	1.74553(30)*	1.47842(15)	1.56322(15)	1.71173(15)
65	Tb		*1.98699(37)*	*1.97586(35)*	*1.77701(32)*	*1.68377(14)*	*1.42285(98)*	*1.50195(80)*	*1.65023(44)*
			1.98753(30)	1.97653(30)	1.77683(44)	1.68303(30)*	1.42232(15)	1.50232(15)	1.64972(15)
66	Dy		*1.91986(35)*	*1.90883(33)*	*1.71052(30)*	*1.62497(12)*	*1.37058(41)*	*1.44500(20)*	*1.59241(33)*
			1.919939(44)	1.908839(44)	1.71065(10)	1.62371(10)*	1.36922(15)	1.44452(15)	1.59162(15)
67	Ho		*1.85606(33)*	*1.84511(31)*	*1.64732(28)*	*1.56818(11)*	*1.31957(28)*	*1.39091(27)*	*1.53614(34)*
			1.856472(15)	**1.845092(17)**	**1.647484(32)**	1.567168(50)*	1.31902(15)	1.39052(15)	1.53682(15)
68	Er		*1.79537(31)*	*1.78449(29)*	*1.58720(26)*	*1.51486(10)*	*1.27145(14)*	*1.33792(26)*	*1.48318(27)*
			1.795701(45)	**1.784481(20)**	**1.587466(86)**	1.51401(13)*	1.27062(15)	1.33862(15)	1.48352(15)
69	Tm		*1.73758(29)*	*1.72677(27)*	*1.52995(24)*	*1.464210(95)*	*1.22612(28)*	*1.28942(27)*	*1.43366(27)*
			1.738003(19)	**1.7267720(70)**	**1.5302410(70)**	1.46402(30)*	1.22502(15)	1.28922(15)	1.43342(15)
70	Yb		*1.68248(29)*	*1.67177(26)*	*1.47538(24)*	*1.416041(89)*	*1.18266(60)*	*1.243391(70)*	*1.3858(10)*
			1.682875(74)	1.671915(59)	1.475672(74)	1.415521(74)*	1.18182(15)	1.24282(15)	1.38622(15)
71	Lu		*1.63031(26)*	*1.61949(24)*	*1.42361(21)*	*1.370061(85)*	*1.14043(22)*	*1.197954(60)*	*1.341053(93)*
			1.630314(74)	1.619534(44)	1.423611(44)	1.370141(44)	1.14022(15)	1.19852(15)	1.34052(15)
72	Hf		*1.58049(25)*	*1.56959(23)*	*1.37419(20)*	*1.326241(78)*	*1.10009(24)*	*1.1550(10)*	*1.2972(14)*
			1.580484(74)	1.569604(74)	1.374121(74)	1.326410(74)	1.1002640(49)	1.1548587(22)	1.2971383(68)
73	Ta		*1.53290(23)*	*1.52194(22)*	*1.32697(19)*	*1.282314(74)*	*1.06152(30)*	*1.11368(14)*	*1.25506(34)*
			1.532953(30)	1.521993(30)	1.327000(44)	1.284559(30)	1.06132(15)	1.11372(15)	1.25532(15)
74	W		*1.48748(22)*	*1.47642(21)*	*1.28188(18)*	*1.244447(70)*	*0.91604(28)*	*1.07431(38)*	*1.21543(99)*
			1.487452(30)	1.4763112(95)	1.281812(13)	1.2443048(98)	1.024685(74)	1.07452(15)	1.21552(15)
75	Re		*1.44399(21)*	*1.43288(19)*	*1.23872(17)*	*1.206487(67)*	*0.98968(21)*	*1.03670(20)*	*1.17673(27)*
			1.443982(74)	1.432922(59)	1.238599(30)	1.206618(59)	0.98941(15)	1.03712(15)	1.17732(15)
76	Os		*1.40238(20)*	*1.39121(18)*	*1.19742(16)*	*1.170095(62)*	*0.95583(36)*	*1.000786(57)*	*1.14002(23)*
			1.402361(74)	1.391231(74)	1.197288(74)	1.16981(12)	0.95581(15)	1.00142(15)	1.14082(15)
77	Ir		*1.36252(19)*	*1.35130(19)*	*1.15786(15)*	*1.135812(72)*	*0.9240(12)*	*0.96675(18)*	*1.10535(22)*
			1.362520(74)	1.351300(44)	1.157827(44)	1.135337(44)	0.92361(15)	0.96711(15)	1.10582(15)
78	Pt		*1.32434(18)*	*1.31308(17)*	*1.11995(14)*	*1.102006(63)*	*0.8933(14)*	*0.93395(27)*	*1.07200(36)*
			1.324340(30)	1.313060(44)	1.119917(30)	1.102017(44)	0.893213(19)	0.9341861(21)	1.0722721(19)
79	Au		*1.28773(17)*	*1.27643(16)*	*1.08359(13)*	*1.070479(53)*	*0.86383(45)*	*0.90263(12)*	*1.04009(27)*
			1.287739(44)	1.276419(44)	1.083546(44)	1.070236(44)	0.863683(30)	0.9027409(46)	1.0401625(52)
80	Hg		*1.25261(16)*	*1.24126(15)*	*1.04869(13)*	*1.039584(51)*	*0.83546(43)*	*0.87238(26)*	*1.00919(30)*
			1.25266(10)	1.241219(74)	1.048696(74)	1.03977(10)	0.83531(15)	0.87221(15)	1.00912(15)
81	Tl		*1.21890(15)*	*1.20750(14)*	*1.01519(12)*	*1.01029(20)*	*0.80795(15)*	*0.843512(77)*	*0.97953(25)*
			1.218768(44)	1.207408(59)	1.015145(59)	1.010325(44)	0.80811(15)	0.84341(15)	0.97931(15)
82	Pb		*1.18651(15)*	*1.17507(14)*	*0.98298(11)*	*0.98221(19)*	*0.78172(24)*	*0.81575(18)*	*0.95113(22)*
			1.186498(74)	1.175028(30)	0.982925(44)	0.98222(10)	0.7818404(49)	0.8157395(16)	0.9511590(22)

* These values are for the unresolved $L\beta_2$ and $L\beta_{15}$ emission lines.

Table 4.2.2.5. *Wavelengths of L-emission lines and L-absorption edges in Å (cont.)*

Z	Symbol	A	$L\alpha_2$	$L\alpha_1$	$L\beta_1$	$L\beta_2$	$L_{\rm I}$ abs. edge	$L_{\rm II}$ abs. edge	$L_{\rm III}$ abs. edge
83	Bi	209	*1.15540(14)*	*1.14390(13)*	*0.95205(11)*	*0.95526(18)*	*0.75649(58)*	*0.789102(88)*	*0.92387(11)*
			1.155377(15)	1.143877(30)	0.951992(13)	0.955194(59)	0.75711(15)	0.78871(15)	0.92341(15)
84	Po	209	*1.12549(13)*	*1.11393(12)*	*0.92228(10)*	*0.92932(18)*	*0.7332(13)*	*0.76325(13)*	*0.897554(85)*
			1.125497(74)	1.113877(59)	0.92201(30)	0.929384(74)			
85	At	210	*1.09670(13)*	*1.08510(12)*	*0.893639(96)*	*0.90444(17)*		*0.73868(13)*	
			1.096726(74)	1.085016(74)	0.89350(13)				
86	Rn	222	*1.06900(12)*	*1.05735(11)*	*0.866054(91)*	*0.88055(15)*		*0.71511(13)*	
			1.069006(74)	1.057246(74)	0.86606(13)				
87	Fr	223	*1.04232(11)*	*1.03063(11)*	*0.839482(86)*	*0.85751(15)*		*0.69240(13)*	*0.8251(27)*
			1.042316(74)	1.030505(74)	0.83941(13)	0.8580(30)			
88	Ra	226	*1.01662(11)*	*1.00489(10)*	*0.813866(82)*	*0.83533(16)*	*0.64449(15)*	*0.67077(12)*	*0.802768(44)*
			1.016575(74)	1.004745(74)	0.813762(74)	0.835383(74)	0.64451(15)	0.67071(15)	0.80281(15)
89	Ac	227	*0.99185(11)*	*0.980070(98)*	*0.789163(78)*	*0.81406(14)*		*0.64970(13)*	
			0.991795(74)	0.979945(74)	0.78904(13)				
90	Th	232	*0.96798(10)*	*0.956154(94)*	*0.765343(75)*	*0.79354(13)*	*0.60569(11)*	*0.62966(11)*	*0.760637(99)*
			0.9679082(23)	0.9560826(15)	0.7652610(14)	0.7935516(15)	0.60591(15)	0.62991(15)	0.76071(15)
91	Pa	231	*0.944896(96)*	*0.933002(90)*	*0.742301(71)*	*0.77321(12)*	*0.58759(12)*	*0.610354(92)*	*0.740958(97)*
			0.944834(74)	0.932854(74)	0.742331(74)	0.77371(15)			
92	U	238	*0.922622(93)*	*0.910674(86)*	*0.720056(68)*	*0.75462(12)*	*0.569885(39)*	*0.591930(66)*	*0.722319(52)*
			0.922572(13)	0.910653(13)	0.719995(12)	0.754692(13)	0.56951(15)	0.59191(15)	0.72231(15)
93	Np	237	*0.901230(88)*	*0.889223(83)*	*0.698624(65)*	*0.73623(11)*			
			0.901059(13)	0.889141(13)	0.698488(13)	0.736241(13)	0.55239(34)	0.57368(37)	0.704136(20)
94	Pu	244	*0.880355(85)*	*0.868290(79)*	*0.677776(60)*	*0.71848(11)*			
							0.53651(15)	0.55721(15)	0.68671(15)
95	Am	243	*0.860288(84)*	*0.848190(81)*	*0.657686(59)*	*0.70134(10)*			
96	Cm	248	*0.840918(80)*	*0.828776(78)*	*0.638265(56)*	*0.684815(98)*			
97	Bk	249	*0.822159(76)*	*0.809987(69)*	*0.619449(53)*	*0.668638(94)*			
							0.49060(49)	0.50851(52)	0.63748(98)
98	Cf	250	*0.803608(73)*	*0.791421(66)*	*0.601005(50)*	*0.652873(89)*			
							0.476569(92)	0.493804(98)	0.62300(19)
99	Es	251	*0.786043(70)*	*0.773837(63)*	*0.583354(49)*	*0.638227(82)*			
100	Fm	254	*0.769077(67)*	*0.756843(60)*	*0.566272(47)*	*0.623826(82)*			
			0.76904(62)	0.75674(60)	0.56619(34)	0.62369(41)	0.44966(13)	0.46534(12)	0.59414(20)

* These values are for the unresolved $L\beta_2$ and $L\beta_{15}$ emission lines.

4.2.2.12. *Structure and format of the summary tables*

Table 4.2.2.4 summarizes the theoretical and experimental results for prominent *K*-series lines and the *K*-absorption edge. For the emission lines, the upper number (in italics) is the theoretical estimate for this line and the lower number is the experimentally measured value (1) from Table 4.2.2.1 or (2) from the Bearden database or a reference that appeared after the Bearden database corrected to the optically based scale. For the *K* absorption edge, the upper number (also in italics) was obtained by combining emission lines and photoelectron spectroscopy (see Subsection 4.2.2.7), and the lower number is the experimentally measured value (1) from Table 4.2.2.3 or (2) from the Bearden database or a reference that appeared after the Bearden database corrected to an optically based scale. For the experimental emission and absorption entries, bold type is used for wavelengths directly measured on an optically based scale. The numerical values for wavelengths in angstrom units (1 Å = 0.1 nm) are given to a number of significant figures commensurate with their estimated uncertainties, which appear in parentheses after each theoretical and experimental value.

Figure 4.2.2.1 shows plots of the relative deviation between theoretical and experimental values for the *K*-series lines and the *K*-absorption edge as a function of *Z*. The error bars shown in the figure are the experimental uncertainties. In general, these plots show good agreement between theory and experiment except in the low-*Z* and high-*Z* regions. At the low-*Z* end of the table, the particular calculational approach used is not optimum, and the experimental data are suprisingly weak. At the high end, experimental data have rather large uncertainties, and thus do not provide an accurate test of the theory.

Table 4.2.2.5 summarizes the theoretical and experimental results for prominent *L*-series lines and the *L*-absorption edges. The experimental database of high-accuracy emission data is much more limited than was the case for the *K* series, and there have been very few high-accuracy edge-location measurements. The format of this table is similar to that of Table 4.2.2.4. For the emission lines, the upper number (in italics) is the theoretical estimate for this line, and the lower number is the experimentally measured value. Numbers in bold type were directly measured on the optical scale (see Table 4.2.2.2), and numbers in normal type are from the Bearden database or a reference that appeared after the Bearden database corrected to an optically based scale. For the *L*-absorption edges, the upper number (also in italics) is obtained by combining emission lines and photoelectron spectroscopy (see Subsection 4.2.2.7) and the lower number is the experimentally measured value. The numbers in bold type

Table 4.2.2.6. *Wavelength conversion factors*

Numbers in parentheses are standard uncertainties in the least-significant figures.

	Cu $K\alpha_1$	Mo $K\alpha_1$	W $K\alpha_1$
λ (Å)	1.54059292(45)	0.70931713(41)	0.20901313(18)
λ (Å*)	1.540562(3)	0.709300(1)	0.2090100
1 kxu	1.537400	0.707831	
Å*/Å	1.0000201(20)	1.0000242(22)	1.00001498(86)
kxu/Å	1.00207683(29)	1.00209955(58)	

are recent measurements by Kraft, Stümpel, Becker & Kuetgens (1996), and the numbers in normal type are from the Bearden database or a reference that appeared after the Bearden database corrected to an optically based scale. Figure 4.2.2.2 shows relative deviations between the theoretical and experimental values for most of the tabulated data. The error bars shown in the figure are the experimental uncertainties.

4.2.2.13. *Availability of a more complete X-ray wavelength table*

This article and the accompanying X-ray wavelength tables are an up-dated version of the contribution to the *International Tables for Crystallography*, Volume C, 2nd edition that was published in 1999. This article has been subject to more critical review and analysis and the data are consistent with the most recent adjustment of the fundamental physical constants (Mohr & Taylor, 2000). We believe that these data represent a significant improvement in consistency, coverage and accuracy over previously available resources. The results presented here are a subset of a larger effort that includes all *K*- and *L*-series lines connecting the $n = 1$ to $n = 4$ shells. The more complete table has been submitted for archival publication and will be made avaialble on the NIST Physical Reference Data web site. Electronic publishing of this resource will provide a convenient data resource to the scientific community that can be more easily up-dated and expanded.

4.2.2.14. *Connection with scales used in previous literature*

In order to compare historical data for X-ray spectra with the results in the present tabulation, certain conversion factors are needed. As discussed in the introduction, the principal units found in the literature are the xu and the Å* unit. There is the additional complication that there were several different definitions in use at various times and at the same time in different laboratories. For the convenience of the reader, we summarize in Table 4.2.2.6 the main conversion factors needed. The numerical values for the wavelengths in Å can be converted to energies in electron volts by using the conversion factor 12 398.41857 (49) eV Å (Mohr & Taylor, 2000).

Our current efforts owe their inception to the encouragement of the late A. J. C. Wilson, who persistently communicated the need for an updated wavelength resource for the crystallographic community. The larger effort evolved at NIST with the support of the Standard Reference Data Program as established with the help of the late Jean Gallagher, and sustained by the program's current Director, John Rumble. Early phases of the preparation of this material benefited from the efforts of John Schweppe. Cedric Powell supplied valuable advice in the area of electron binding energies. We are particularly grateful to the Editor, E. Prince, for his help and patience in the development of these wavelength tables. Richard Deslattes died between the first publication of this article and this revision. This work would not have been possible without his dedication to this project over more than a decade. The earlier wavelength table of the late J. A. Bearden, under whom one of the present authors (RDD) studied, was a significant influence on this project.

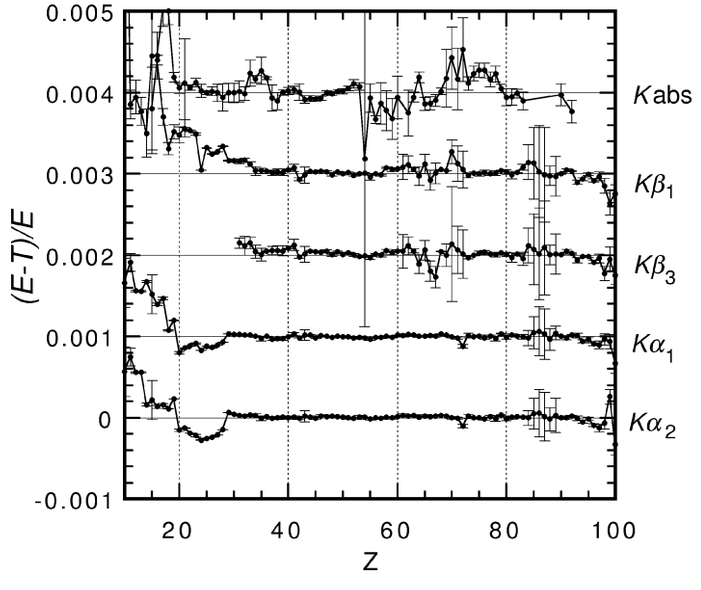

Fig. 4.2.2.1. Relative deviations between theoretical and experimental results for *K*-series spectra. The topmost data set concerns the *K*-edge location, while the other data sets, beginning at the bottom, refer to the $K\alpha_2$, $K\alpha_1$, $K\beta_3$ and $K\beta_1$, respectively. The ordinate scales have been displaced for clarity by the indicated multiples of 0.001.

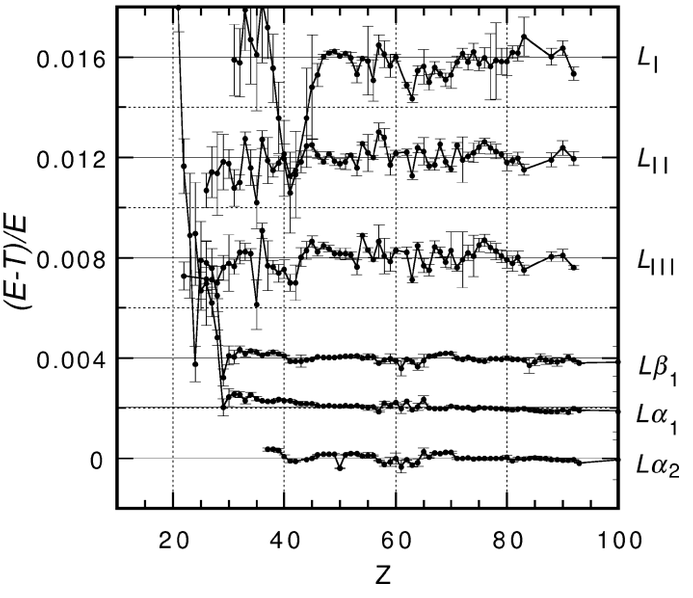

Fig. 4.2.2.2. Comparison of *L*-series data with experiment for the indicated range of *Z*. Indicated data, beginning at the bottom, refer to the $L\alpha_2$, $L\alpha_1$, and $L\beta_1$ emission lines and the L_{III}, L_{II}, and L_I absorption edges. For clarity, the plots have been displaced vertically by multiples of 0.002 for the emission lines and 0.004 for the absorption edges.